fire

MDPI

Article

Microwave Chemical Looping Synergistic Gasification of Polypropylene Plastic and Water Hyacinth

Fengxia An [1,2], Delu Chen [2], Wenli Mao [2], Ying Yu [1], Danyang Shao [2], Zhaoping Zhong [2,*] and Xiaojia Wang [2,*]

[1] China Energy Science and Technology Research Institute Co., Ltd., Nanjing 210023, China; 20080589@ceic.com (F.A.); 20036288@ceic.com (Y.Y.)
[2] Key Laboratory of Energy Thermal Conversion and Control of Ministry of Education, School of Energy and Environment, Southeast University, Nanjing 210096, China; deluchen@seu.edu.cn (D.C.); wenlimao@seu.edu.cn (W.M.); danyangshao@seu.edu.cn (D.S.)
* Correspondence: zzhong@seu.edu.cn (Z.Z.); xiaojiawang@seu.edu.cn (X.W.)

Abstract: The microwave chemical looping synergistic gasification characteristics of municipal solid waste polypropylene plastic and the organic solid waste water hyacinth are experimentally investigated in this study. In addition, the characterizations of oxygen carriers before and after the reaction are combined to analyze the evolution of the microscopic morphology of oxygen carriers and the changes in the relative contents of each valence state of Fe and O elements. The results show that an increase in the water hyacinth mixing ratio presents positive effects on tar cracking and a slight negative effect on syngas yield. At the water hyacinth mixing ratio of 75%, the cold gas efficiency and carbon conversion can reach maximum values of 77.64% and 69.9%, respectively. The H_2 yield and H_2/CO ratio in syngas can be also improved to 0.34 Nm^3/kg and 1.62, respectively. In addition, a minimum tar yield of 0.133 g/g (fuel) can be obtained at this mixing ratio. Moreover, the addition of water hyacinth has a continuous increase effect on monocyclic aromatic hydrocarbon (MAH) products of tar, and a continuous decrease effect on naphthalene and bicyclic aromatic hydrocarbons (NAH) products. This work explores the synergistic properties of organic waste plastics and agroforestry wastes during microwave chemical looping gasification, which is a useful exploration for solving the environmental problems caused by waste materials and agroforestry wastes as well as realizing the resourceful utilization of solid wastes.

Keywords: microwave chemical looping; synergistic gasification; oxygen carrier; polypropylene plastic; water hyacinth

check for updates

Academic Editor: Jiajian Zhu

Received: 1 December 2024
Revised: 4 January 2025
Accepted: 10 January 2025
Published: 12 February 2025

Citation: An, F.; Chen, D.; Mao, W.; Yu, Y.; Shao, D.; Zhong, Z.; Wang, X. Microwave Chemical Looping Synergistic Gasification of Polypropylene Plastic and Water Hyacinth. *Fire* **2025**, *8*, 76. https://doi.org/10.3390/fire8020076

Copyright: © 2025 by the authors. Licensee MDPI, Basel, Switzerland. This article is an open access article distributed under the terms and conditions of the Creative Commons Attribution (CC BY) license (https://creativecommons.org/licenses/by/4.0/).

1. Introduction

The development of high-efficiency thermal treatment technology that converts organic solid wastes with low-grade energy into high-grade clean energy is of great significance in meeting the major needs of carbon neutrality, mitigating environmental pollution, and realizing the resource utilization of organic solid wastes [1–4]. Gasification is an effective treatment method to convert organic solid wastes into combustible gases, such as H_2, CO, and CH_4. However, traditional gasification technology has low efficiency and high energy consumption and is accompanied by the generation of tar as a by-product, which poses a threat to production safety. Chemical looping gasification (CLG), as a novel type of gasification technology with important prospects, can realize the gradient utilization of chemical energy, reduce energy consumption, and improve the quality of syngas production [5–10]. In the CLG process, a kind of oxygen carrier circulates between an air reactor

and a gasification reactor to gasify the fuel. The oxygen carrier can release lattice oxygen in the gasification reactor to convert biomass into combustible syngas. Meanwhile, the oxygen carrier can transfer heat from the air reactor to the gasification reactor to achieve the self-balancing of heat in the system. In addition, the metal oxides contained in the oxygen carrier itself can be used as a catalyst to promote the conversion of fuels to combustible gases and the decomposition of tars during the gasification process. Microwave chemical looping gasification technology can effectively improve the gasification rate, and its rapid and uniform heating characteristics are conducive to the heating and cracking of tar, further improving the efficiency and quality of syngas production [11–17].

Studies have shown that there are certain synergies between the gasification of two different organic solid waste materials mixed in different proportions [18,19]. Compared with organic solid waste alone gasification reaction, co-gasification of agricultural and forestry wastes and organic municipal solid wastes is a highly efficient way to realize resource utilization [20–22]. Agroforestry wastes are widely available and homogeneous, usually containing alkali and alkaline earth metals, which can be used as inexpensive natural catalysts to reduce the additional addition of catalysts in gasification technologies and to enhance catalytic gasification reactions, with the promise of targeted enhancement of specific products and gasification characteristics [23,24]. Yang et al. [25] investigated the interaction of high-calorific value plastics and rice straw during hybrid gasification. The results showed that synergistic effects exist when the performance of the hybrid fuel is higher than the linear sum of the fuel-weighted averages and is enhanced with higher plasticity ratios in the hybrid fuel. Zhang et al. [26] investigated the co-pyrolysis characteristics of a mixture of sludge and rice straw. They found that when the sludge content increased, the gas yield decreased significantly and the gas composition changed significantly. Torquato et al. [27] studied the mixed gasification characteristics of bagasse and sludge mixtures. The results showed that increasing bagasse content can promote the calorific value of the gas produced. Lahijani et al. [28] studied the co-gasification characteristics of palm or almond husk and tires. They observed that a 50:50 mixing ratio of palm or almond husk to tires can increase the gasification conversion 10 and 5 times, respectively, when compared to pure tire gasification. Presently, there is a lack of corresponding research on the chemical looping gasification characteristics of a variety of organic wastes heated by microwave. Since microwave heating differs from conventional heaters [29], it is necessary to explore the microwave chemical looping gasification characteristics of different wastes.

Water hyacinth is an exotic bio-invasive species due to its extremely fast growth and reproduction ability, which makes it easy for water hyacinth to escape from the planting area. Since water hyacinth itself has no natural enemies, its invasion will seriously jeopardize local aquatic organisms, aquatic plants, and aquaculture industries. As white pollution has increased in recent years, plastic waste cannot be decomposed and incineration produces toxic pollutants such as dioxins, so there is an urgent need for a way to utilize plastic waste in a cleaner way. Polypropylene (PP) plastics are a typical plastic waste, and their high hydrogen content makes them widely used in gasification research.

Therefore, this study selects PP plastic and water hyacinth as the fuels and adopts a natural iron ore as the oxygen carrier. The microwave chemical looping synergistic gasification characteristics of the municipal solid waste PP plastic and the organic solid waste water hyacinth are experimentally investigated. In addition, combined with the characterizations before and after the reaction, the synergistic mechanism for microwave chemical looping gasification is further explored. This work aims to provide a solution to the environmental problems caused by PP and agroforestry wastes while realizing the resource utilization of waste plastics and agroforestry wastes through the new microwave heating technology coupled with chemical looping technology.

2. Experimental Materials and Methods

2.1. Experimental Materials, Reagents and Equipments

2.1.1. Basic Experimental Materials

Prior to the experiment, the water hyacinth and PP plastic (Maoming Petrochemical Company, Maoming, China) were first dried in the oven at 120 °C for 24 h and then crushed for storage. The prepared fuel samples for the test are shown in Figure 1, and the elemental analysis results are shown in Table 1. The iron ore oxygen carrier mainly contained Fe_2O_3 (54.49%), SiO_2 (27.31%), Al_2O_3 (3.69%), CaO (3.43%) and MgO (2.65%). It was crushed first and then calcined at a high temperature of 1000 °C in a muffle furnace for 6 h.



Figure 1. Fuel test sample diagram: (**a**) water hyacinth, (**b**) PP plastic.

Table 1. Elemental analysis results of water hyacinth and PP plastics (air-dried basis, %).

Material	C	H	O	N	S
Water hyacinth	28.55	4.03	32.30	2.04	0.81
PP plastic	83.61	12.82	3.57	0	-

2.1.2. Major Experimental Reagents

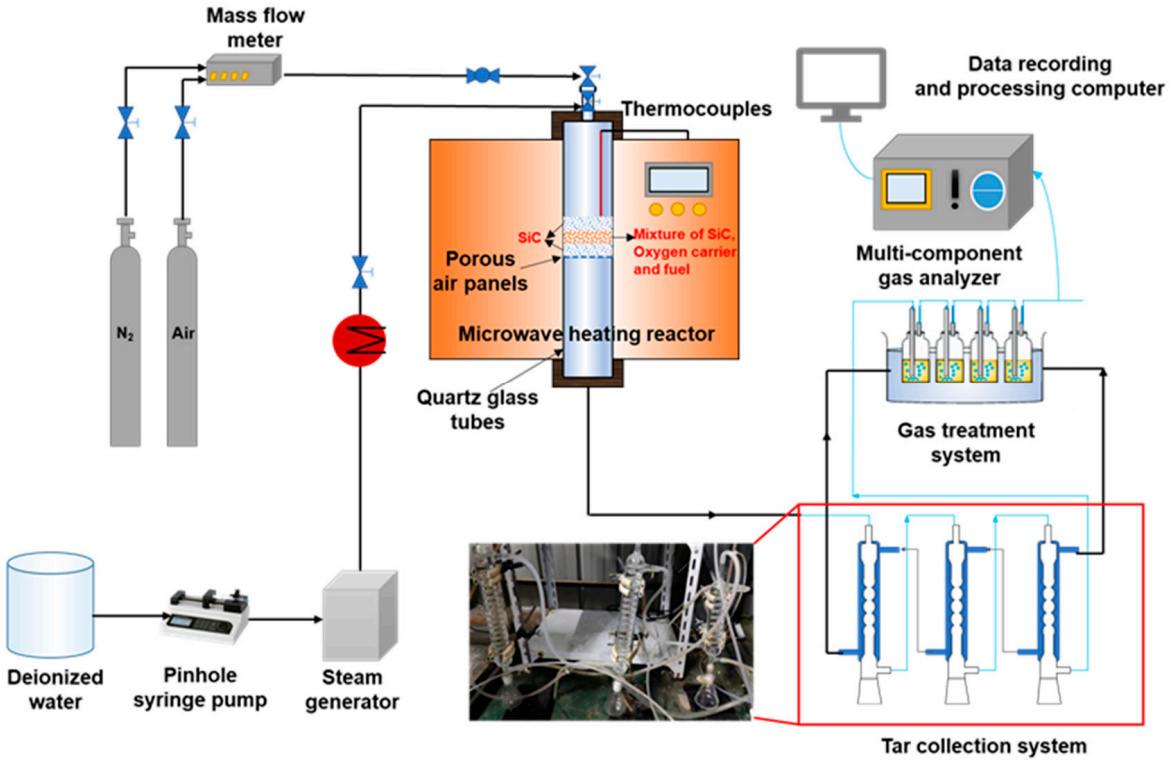
High-purity nitrogen (≥99.99%), isopropanol (AR), anhydrous calcium chloride (AR), color-changing silicone (L), and deionized water (self-prepared) were used.

2.1.3. Major Experimental Equipment

The experiment used the following: gas mass flowmeters (range: 0–2000 mL/min), a gas analyzer (CH_4: 0–50%, H_2: 0–50%, CO: 0–50%, CO_2: 0–50%, O_2: 0–25%), a steam generator (temperature rise range: 0–400 °C), an electronic balance (range: 0–200 g, accurate: 0.001 g), a crusher (crushing range: 70–300 mesh), a water pump (head: 3 m), and a microwave reactor (frequency: 2.45 GHz, power range: 0–1000 W).

2.2. Experimental Device and Process

The fixed bed experimental device for microwave chemical looping gasification mainly consists of a microwave reactor, feed system, gas treatment system, online analysis system, and tar collection system (as shown in Scheme 1). The detailed description of the reactor system can be found elsewhere [30].



Scheme 1. Microwave chemical looping gasification test apparatus.

Before each test, a porous stainless steel air distribution plate is placed in the middle of the quartz tube to carry the material. The bed material structure in the experiment is a three-layer structure, which is divided into silicon carbide (SiC) bottom layer, iron ore oxygen carrier, fuel, SiC intermediate mixed layer, and SiC top layer. The bed temperature is measured by a type K thermocouple and controlled by a proportion integral differential (PID) program. N_2 is introduced into the system to purge the piping system for 5 min after loading the material, in order to ensure that there is no residual reactive gas. Afterwards, the N_2 flow rate is set to 600 mL/min, and the reaction target temperature and microwave heating power are set in the microwave reactor. Finally, the pinhole injection pump and microwave reactor are started for reaction. In the process of the experiment, microwave chemical looping synergistic gasification will be maintained for 30 min. The syngas generated during the test is successively passed through the tar collection system, the washing cylinders (isopropyl alcohol, water, calcium chloride) in the ice bath water cooling unit, and finally the multi-component gas analyzer.

The collected tar is heated and stirred with a magnetic stirrer so that the volume of the solution is reduced to less than 50 mL. The solution is shaken in an ultrasonic oscillator for 30 min and then left to stand for 30 min. The upper layer of the liquid is absorbed with a pinhole syringe and then filtered through a 0.2 μm PTFE filter tip into a chromatographic volume bottle, which is then scanned with a gas chromatography–mass spectrometry (GC-MS) device.

2.3. Experimental Conditions

The experiments are carried out under the conditions of 900 °C for the reaction temperature and 3.49 for the mass ratio of oxygen carrier to fuel. The mixing ratios of water hyacinth and PP plastic are set as 0:100%, 25%:75%, 50%:50%, and 75%:25%, which are labeled 0, 0.25, 0.5, and 0.75, respectively.

2.4. Data Processing

The total gas yield and each single gas component yield are calculated by Equations (1) and (2). The relative portion of a single gas component in the syngas and the lower heating value of syngas can be further obtained, as shown in Equations (3) and (4):

$$Y_i = \int_0^t \frac{V_{N_2} \times X_i \times 273}{m_0 \times (1 - \sum X_i) \times 288} d_t \quad (1)$$

$$Y_g = \sum Y_i \ (\mathrm{i} = \ \mathrm{H_2, CH_4, CO, CO_2}) \quad (2)$$

$$P_i = \frac{Y_i}{Y_g} \times 100\% \quad (3)$$

$$LHV = 0.108P_{H_2} + 0.359P_{CH_4} + 0.126P_{CO} \quad (4)$$

where Y_i is the yield of each single gas component in the syngas and $\mathrm{Nm^3/kg}$ fuel, and it is obtained by integrating the component change curves obtained from the analyzer; 273 and 288 represent the temperatures of 273 K and 288 K, respectively. V_{N_2} is the N_2 flow rate at the inlet under room temperature, $\mathrm{m^3/s}$. X_i is the volume fraction of each single gas component measured online by the gas analyzer, %. m_0 is the total mass of fuel introduced to the reactor, kg. Y_g is the total gas yield, $\mathrm{Nm^3/kg}$ fuel. P_i is the relative portion of each single gas component in the gas product, %. LHV is the lower heating value of the gas product, $\mathrm{MJ/Nm^3}$.

In order to reflect the gasification reaction characteristics, H_2/CO ratio, CO/CO_2 ratio, carbon conversion, and cold gas efficiency are often used as the gasification indicators, as shown in Equations (5)–(8):

$$H_2/CO = \frac{Y_{H_2}}{Y_{CO}} \quad (5)$$

$$CO/CO_2 = \frac{Y_{CO}}{Y_{CO_2}} \quad (6)$$

$$\eta_c = \frac{12 \times m_0 \times \left(Y_{\mathrm{CO}} + Y_{CO_2} + Y_{CH_4}\right)}{22.4 \times f_c} \times 100\% \quad (7)$$

$$CGE = \left(LHV \times Y_g\right)/q_0 \times 100\% \quad (8)$$

where H_2/CO is the H_2/CO ratio in the gas product. CO/CO_2 is the CO/CO_2 ratio in the gas product. η_c is the carbon conversion, %. f_c is the mass fraction of carbon in the added fuel, %. CGE is the cold gas efficiency, %. q_0 is the low calorific value of the introduced fuel, MJ/kg.

2.5. Reactions Involving Tar

Reactions involving tar are shown in Formulas (9) to (13).

$$\text{Solid fuel} \overset{\text{microwave heating}}{\rightarrow} \text{char} + \text{tar} + \text{syngas} \ (\mathrm{H_2, CO, CO_2, CH_4}, \text{etc.}) \quad (9)$$

$$\text{Tar cracking reaction} \quad \text{tar} \rightarrow \text{coke} + \text{syngas}, \ \Delta\mathrm{H} > 0 \quad (10)$$

$$\text{Dehydrogenation reaction} \quad \text{tar} \rightarrow \mathrm{xC}_n\mathrm{H}_m + \mathrm{yH_2}, \ \Delta\mathrm{H} > 0 \quad (11)$$

$$\text{Tar reforming reaction} \quad \text{tar} + \mathrm{H_2O} \rightarrow \mathrm{CO_2} + \mathrm{H_2} + \mathrm{CO} + \mathrm{C_mH_n} + \cdots \quad (12)$$

$$\text{Oxidation reaction of tar substances} \quad \text{tar} + \mathrm{Fe_2O_3} \rightarrow \mathrm{CO_2} + \mathrm{CO} + \mathrm{H_2} + \mathrm{H_2O} + \mathrm{C_mH_n} + \cdots \quad (13)$$

3. Results and Discussions

3.1. Influence of Water Hyacinth Mixing on the Gasification Characteristics

3.1.1. Evolution of Gas–Liquid–Solid Products

The effects of the mixing of water hyacinth with PP plastic on the gas–liquid–solid three-phase mass yields are shown in Figure 2. The results show that the tar production can be effectively decreased from 0.21 to 0.13 g/g with the increase in the water hyacinth mixing ratio from 0 to 0.75. On the other hand, the syngas yield slightly decreases from 0.78 to 0.69 g/g. Moreover, the mass yield of char continues to increase from 0.01 to 0.18 g/g with the increase in mixing ratio. Due to the high volatile content and low contents of ash and fixed carbon, most of the selected PP plastic can be transformed into gas products in the early pyrolysis stage of chemical looping gasification, and thus semi-coke gasification in subsequent stages is not required. As a result, there is almost no incomplete char component in the product for the condition of pure PP plastic [31].

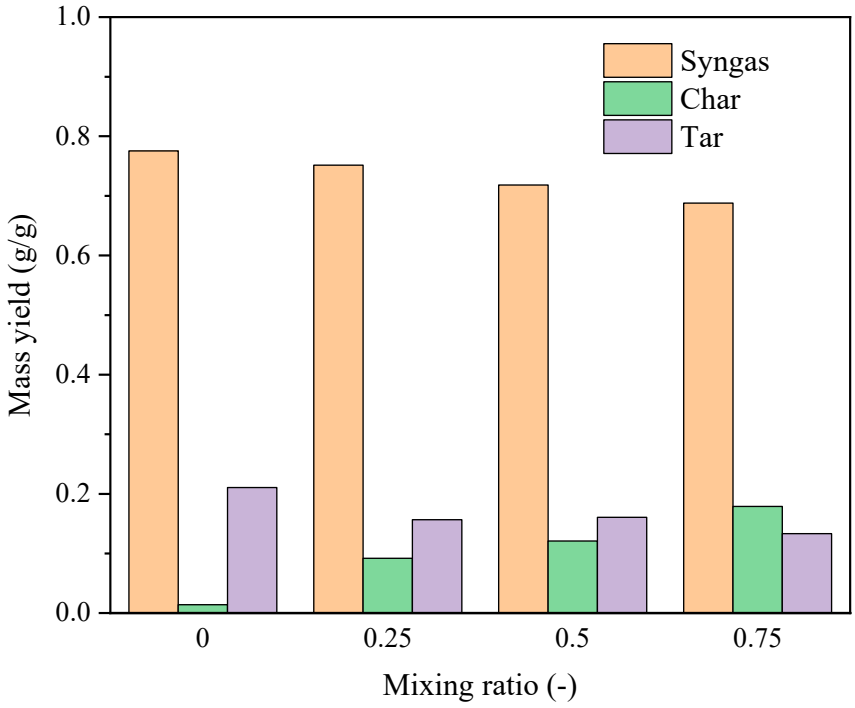


Figure 2. Effect of water hyacinth mixing ratio on gas–liquid–solid yields.

3.1.2. Syngas Composition Distributions

Figures 3 and 4 display the effect of the water hyacinth mixing ratio on the syngas yield and composition distribution. The results show that with the increase in water hyacinth content, the total gas yield keeps decreasing from 1.05 Nm^3/kg for pure PP plastic to 0.9 Nm^3/kg with the mixing ratio of 0.75. This is mainly because the decrease in high-volatile PP plastic lowers the overall volatile fraction of the mixed fuel. Thus, in the early pyrolysis stage of chemical looping gasification, fewer gas products are released, which reduces the total gas yield [31]. Accordingly, the yield of CH_4 is also obviously reduced from 0.41 Nm^3/kg for pure PP plastic to 0.21 Nm^3/kg for the mixing ratio of 0.75. However, the CO yield remains almost constant. Moreover, the H_2 yield slightly increases with the increasing water hyacinth content, reaching a maximum of 0.34 Nm^3/kg at the condition of 0.75 mixing ratio. This is mainly because plastics are hydrocarbon polymers formed by addition polymerization, and PP plastics are formed by adding methyl molecules (-CH_3) to conventional hydrocarbon structures. Thus, in the pyrolysis stage, a large number of -CH_3 free radicals are generated, which makes it easier to generate hydrocarbons including

CH_4. Afterward, a series of reforming reactions occur with steam, and a series of oxidation reactions occur with lattice oxygen released by the iron ore oxygen carrier, resulting in the generation of CO and CO_2.

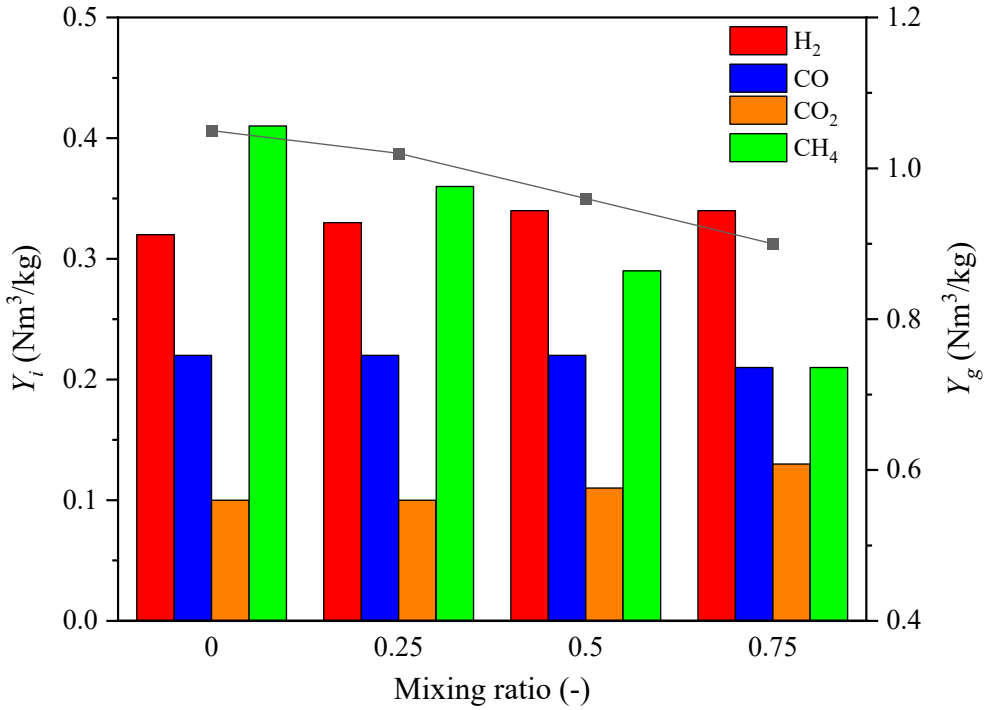


Figure 3. Effect of water hyacinth mixing ratio on syngas yield.

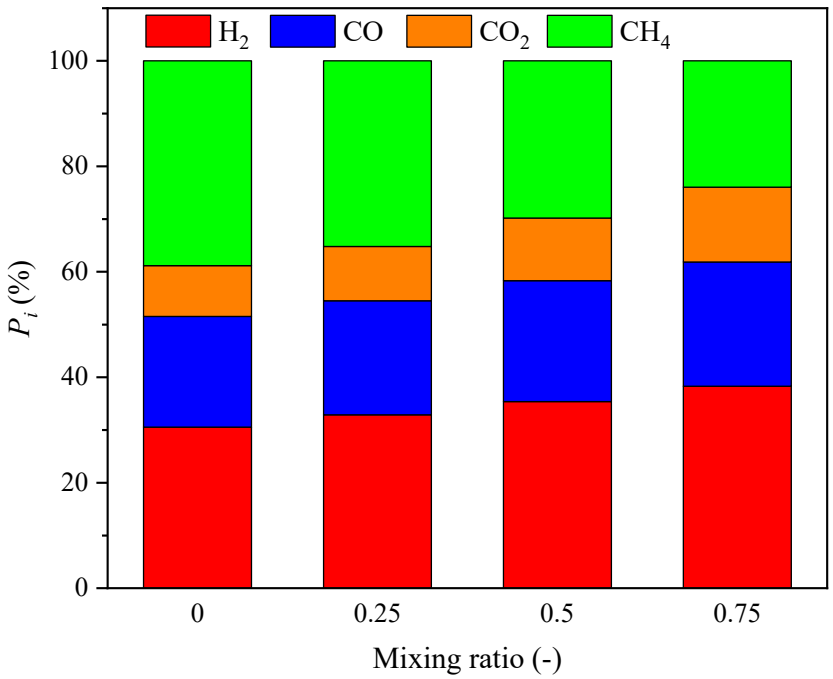


Figure 4. Effect of water hyacinth mixing ratio on syngas composition distribution.

3.1.3. Gasification Characteristics

Figure 5 shows the effect of water hyacinth mixing on gasification reaction characteristics. It can be seen that with the increase in the water hyacinth mixing ratio from 0 to 0.75, the cold gas efficiency and carbon conversion are greatly promoted from 50.70% and 46.70% to 77.64% and 69.9%, respectively. This is because water hyacinth contains more organic matter, such as cellulose, hemicellulose, and lignin, and the microwave uniform heating

characteristics lead to the same direction of heat and mass transfer in water hyacinth, which promotes the carbon conversion rate. On the other hand, the lower heating value decreases from 19.89 to 15.71 MJ/Nm^3, which is mainly because of the decrease in CH_4 content.

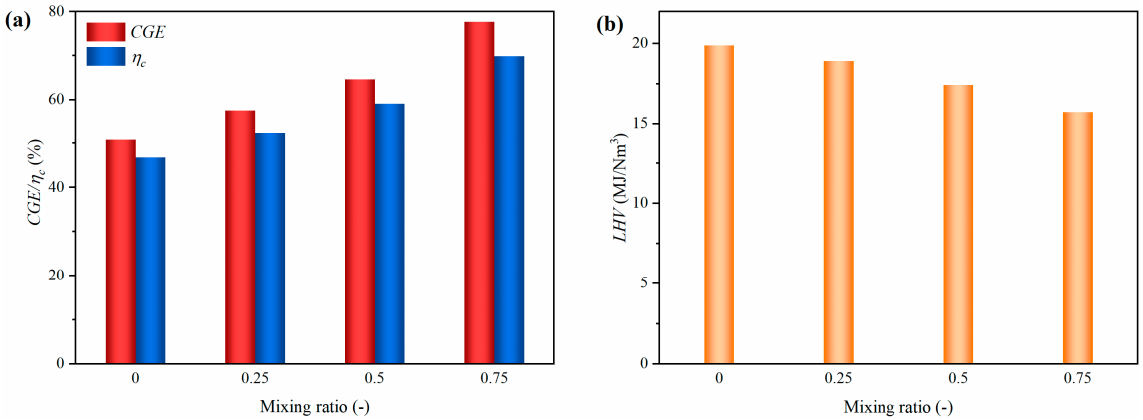


Figure 5. Effect of water hyacinth mixing ratio on cold gas efficiency and carbon conversion (**a**) and lower heating value (**b**).

Figure 6 presents the influence of the water hyacinth mixing ratio on the ratios of H_2/CO and CO/CO_2. From the condition of 0 to 0.75 condition, the H_2/CO ratio in syngas can be improved from 1.46 to 1.62. However, the CO/CO_2 ratio in syngas gradually decreases from 2.18 to 1.67, indicating that the addition of water hyacinth leads to a certain degree of excessive oxidation of the C element to the CO_2 stage, rather than the CO stage.

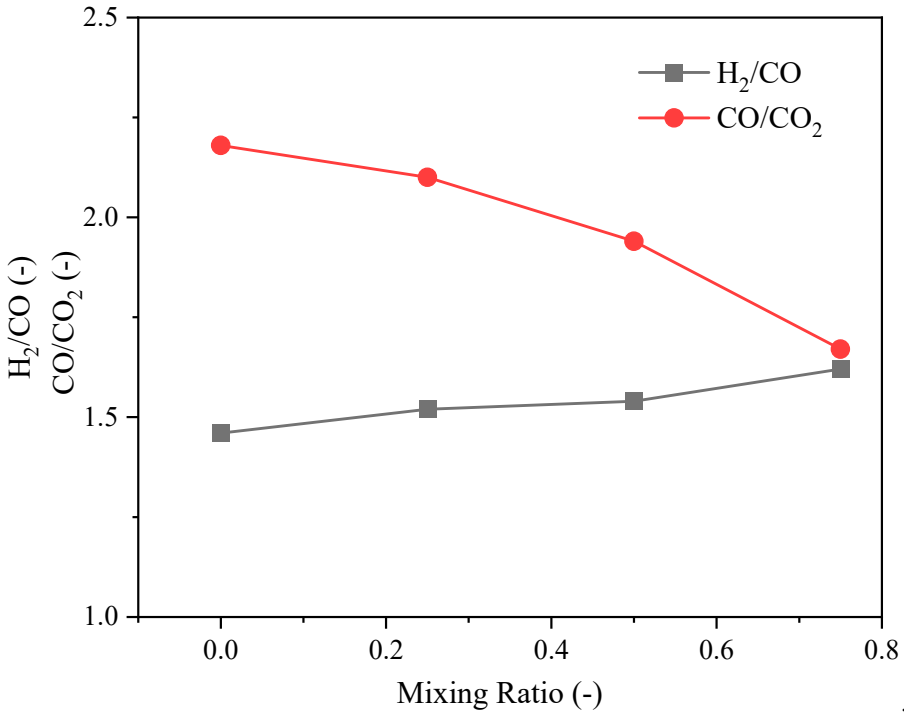


Figure 6. Influence of water hyacinth mixing ratio on the ratios of H_2/CO and CO/CO_2.

The water hyacinth has the characteristics of low carbon content, and hence collaborative treatment with PP plastic can effectively improve the carbon conversion, cold gas efficiency, and hydrogen–carbon ratio of syngas. On a deeper level, the alkali metal and alkaline earth metal components in biomass also promote the reaction rate of plastic waste. The formation of potassium compounds, such as $KAlSiO_4$, $Ca_3Al_2(SiO_4)_3$, and K_2SiO_3, in

the gasification process promotes the gasification rate and synergistic effect of water hyacinth and PP plastic and improves the reactivity of non-activated carbon materials [32]. In turn, PP plastics can provide more active sites for biomass gasification, and thus hydrogen transfers from polymers to biomass-derived free radicals, promoting the development of reaction products towards small-molecule alkane compounds.

3.2. Element Valence States in Oxygen Carrier

Figure 7 shows the XPS characterization results of Fe element valence states in oxygen carriers. The results show that the peak values of Fe^{3+} and Fe^{2+} in the $Fe2p_{3/2}$ orbit are located at the binding energies of 712.66 eV and 710.74 eV, respectively. In the spectrums of oxygen carrier after reaction, Fe^0 metal is formed, and its corresponding spectral peak binding energy is 708 eV, indicating that part of the Fe_2O_3 is reduced to metal Fe during the reaction process.

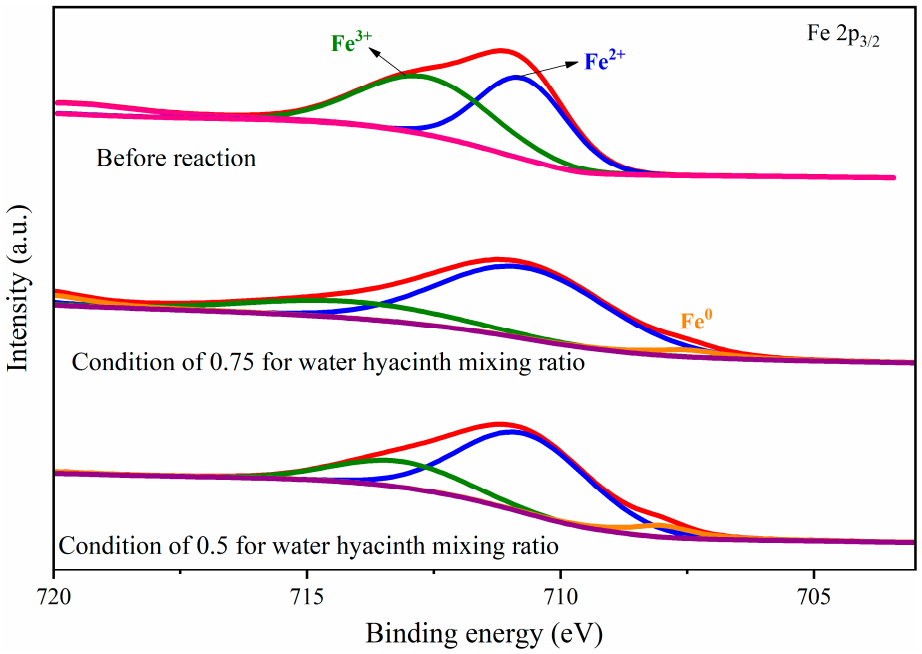


Figure 7. XPS spectrums of Fe element valence states in oxygen carrier.

Table 2 lists the relative content changes of Fe element valence states and shows that in the fresh oxygen carrier, the atomic ratios of Fe^{3+} and Fe^{2+} are 51.77% and 48.23%, respectively, and Fe^0 is not detected. In the condition of 0.75 for the water hyacinth mixing ratio, the atomic ratios of Fe^{3+}, $Fe^{2+,}$, and Fe^0 in the oxygen carrier are 21.22%, 73.86%, and 4.92%, respectively. In the condition of 0.5 for the water hyacinth mixing ratio, the atomic ratios of Fe^{3+}, Fe^{2+}, and Fe^0 in the oxygen carrier are 22.87%, 69.67%, and 7.46%, respectively. The results show that in the oxygen carrier after the reaction, the proportion of Fe^{3+} decreases significantly, while the proportions of Fe^{2+} and Fe^0 increase, indicating that Fe_2O_3 has been gradually reduced to Fe_3O_4, FeO, and Fe.

Table 2. Changes in the relative contents of Fe elemental valence states in oxygen carrier.

Valence State of the Element		Unit	Before Reaction	Mixing Ratio of 0.75	Mixing Ratio of 0.5
$Fe2p_{3/2}$	Fe^{3+}	at%	51.77	21.22	22.87
	Fe^{2+}	at%	48.23	73.86	69.67
	Fe^0	at%	-	4.92	7.46

The XPS characterization results of O element valence states in oxygen carriers are shown in Figure 8, and the relative content changes of each O element valence state are shown in Table 3. The results show that the relative contents of crystal lattice oxygen, chemisorbed oxygen and physical adsorbed oxygen atoms on the surface of fresh oxygen carrier were 29.7%, 41.76%, and 28.53%, respectively. Accordingly, the ratios of crystal lattice oxygen, chemisorbed oxygen, and physical adsorbed oxygen atoms on the surface of the oxygen carrier under the conditions of 0.75 and 0.5 for water hyacinth mixing ratio are 15.65% and 5.86%, 45.66% and 49.07%, and 38.69% and 45.07%, respectively. The results indicate that the oxygen carrier under 0.75 and 0.5 conditions can transform most of the lattice oxygen in the bulk phase into physical adsorption oxygen through oxygen vacancy for the gasification reaction.

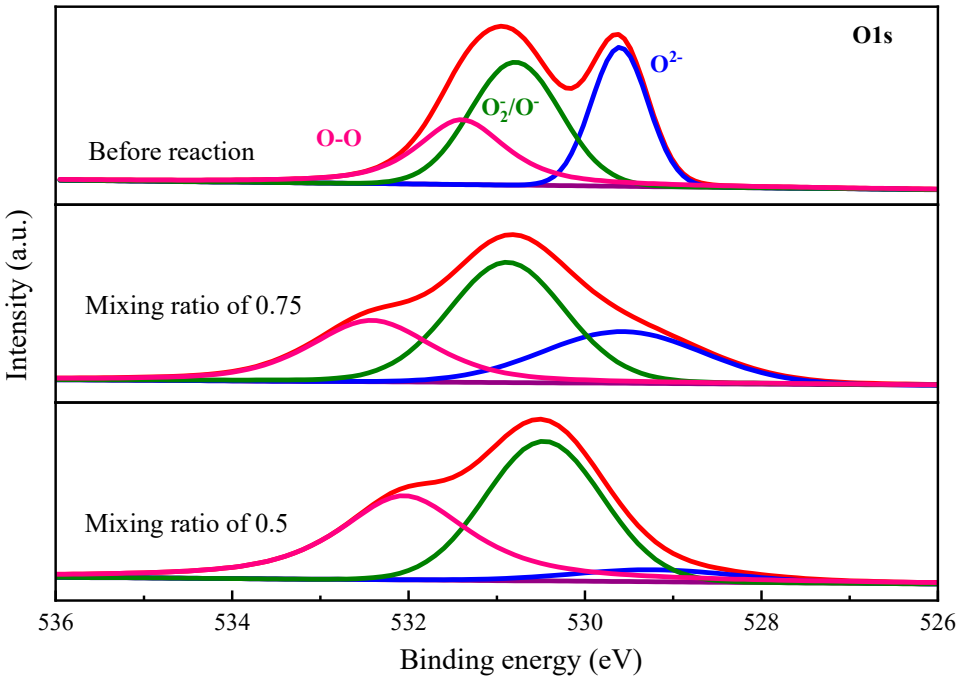


Figure 8. XPS spectrums of O element valence states in oxygen carrier.

Table 3. Changes in the relative contents of O element valence states in oxygen carrier.

Valence State of the Element		Unit	Pre-Reaction	Mixing Ratio of 0.75	Mixing Ratio of 0.5
O1s	O^{2-}	at%	29.70	15.65	5.86
	O^{2-}/O^{-}	at%	41.76	45.66	49.07
	O_2	at%	28.53	38.69	45.07

3.3. Influence of Water Hyacinth Mixing on Tar Characteristics

3.3.1. Variation of Tar Yield Under Different Blending Ratios in Synergistic Gasification

Figure 9 shows the variation in tar yield in synergistic gasification under different blending ratios of water hyacinth. The results show that the tar yield of PP plastic single gasification is 0.211 g/g (fuel). Taking PP plastic single gasification as the basic working condition, the blending of the two fuels exhibits an obvious inhibitory effect on tar generation. When the blending ratio is 25:75 (0.25 working condition), the tar yield is 0.157 g/g (fuel), the decrease in tar yield is 0.054 g/g (fuel), and the cracking rate is 25.6%. When the blending ratio is 50:50 (0.5 working condition), the tar yield is 0.161 g/g (fuel), the decrease in tar yield is 0.050 g/g (fuel), and the cracking rate is 23.7%. When the blending ratio is 75:25 (0.75 working condition), the tar yield is 0.133 g/g (fuel), reaching the minimum

value, the reduction of tar yield is 0.077 g/g (fuel), and the cracking rate is 36.5%. It can be observed that the addition of water hyacinth can bring about an obvious decrease in tar yield in the range of 20–40%. This may be because the hydrocarbons with active free radical sites from random breaks of the original polymer chains in the structure of PP plastic, interact with the hydroxyl fragments from water hyacinth, which reduces the proportion and rate of the aromatic hydrocarbon compounds' generation [33].

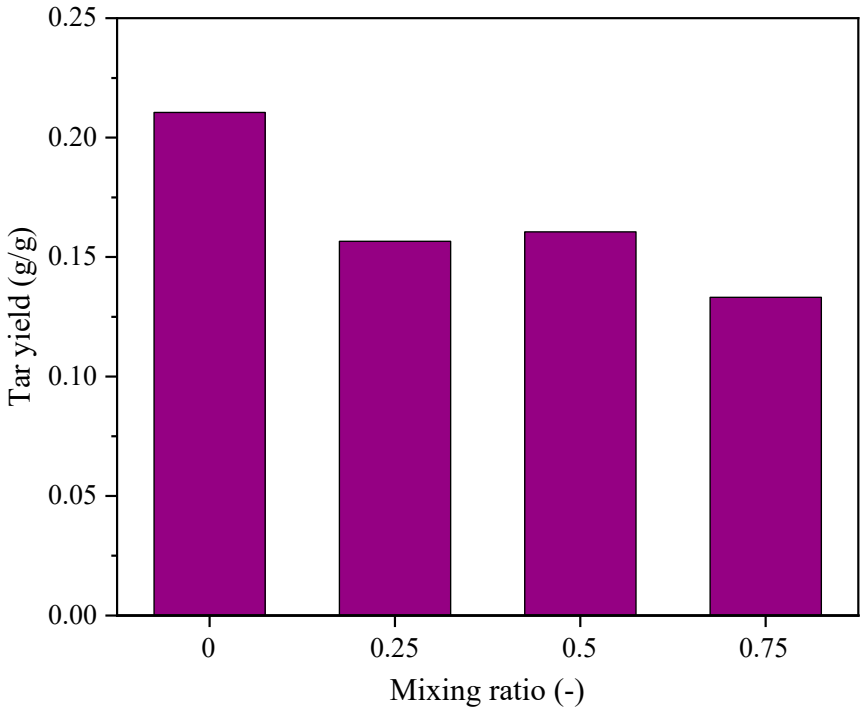


Figure 9. Variation of tar yield under different blending ratios of water hyacinth.

3.3.2. Variation in the Contents of Tar Components Under Different Blending Ratios

Figure 10 shows the variations in the content of tar components under different water hyacinth blending ratios, and Table 4 shows the change in the contents of tar components. The main tar components are monocyclic aromatic hydrocarbon compounds (MAHs), naphthalene and bicyclic aromatic hydrocarbon compounds (NAHs), and polycyclic aromatic hydrocarbon compounds (PAHs). The results show that PAHs products show a decreasing and then increasing trend with the increase in the blending ratio and reach the minimum value of 19.8% under the working condition of 0.5 for water hyacinth mixing ratio. The production of MAHs keeps increasing from 27.4% for PP plastic single gasification to 41.8% for 0.75 water hyacinth mixing ratio, while the production of NAHs decreases continuously from 46.9% to 35.5%. It can be observed that the mixing of water hyacinth brings about different synergistic effects on different tar components. The water hyacinth biomass is rich in a large number of alkali metals and alkaline earth metals, which leads to a synergistic reaction in the co-gasification process [34]. In addition, the mixture of biomass and plastic reduces the H/C atomic ratio of char, which can improve the degree and stability of carbon structure. These factors are helpful to tar cracking and reforming.

In this study, the gasification characteristics at a blending ratio of 0.75 showed the best hydrogen yield (0.34 Nm^3/kg) and the lowest tar yield (0.133 g/g). Table 5 lists the biomass microwave chemical looping gasification characteristics for different feedstocks and oxygen carriers. The comparison of different feedstocks revealed that PP is an excellent feedstock for gas production, but the tar yield is higher [35]. Faced by this issue, this study combines municipal solid waste PP plastic and organic solid waste water hyacinth to explore the effect of mixing ratio on syngas performance and tar removal. It is a meaningful

exploration that the quality of microwave chemical looping gasification can be effectively improved and by-product tar production can be reduced.

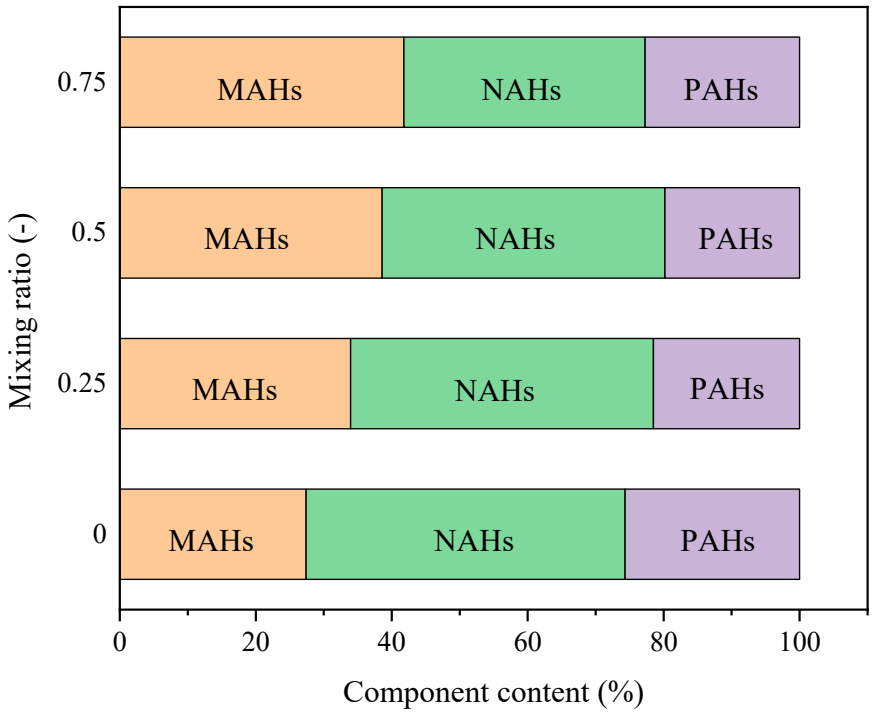


Figure 10. Variation in the contents of tar components under different blending ratios of water hyacinth.

Table 4. Changes in the contents of tar components under different water hyacinth blending ratios.

Tar Components	0	0.25	0.5	0.75
PAHs	25.68	21.52	19.82	22.73
NAHs	46.92	44.54	41.59	35.46
MAHs	27.40	33.94	38.59	41.81

Table 5. Biomass microwave chemical looping gasification characteristics for different feedstocks and oxygen carriers.

Feedstock	Condition	Oxygen Carrier	Gasification Effct	Reference
PP	890 W, 900 °C, air	$NiFe_{20}Ox$	Gas yield = 81.3 mmol/g PP, Tar yield = 23.3 wt.%	[29]
Sugarcane bagasse	880 W, 800 °C, air	Fe_3O_4	Syngas yield (wt.%) = 88.23%	[35]
Water hyacinth: PP = 0.75	900 °C, 1000 W, steam = 0.1 mL/min	Iron Ore	η_c = 69.9%, CGE = 77.64%, H_2 yield = 0.34 Nm^3/kg, tar yield = 0.133 g/g	This Study

4. Conclusions

In this study, the microwave chemical looping synergistic gasification characteristics of polypropylene plastic and water hyacinth are experimentally investigated. In summary, tar cracking was promoted and syngas yield was slightly reduced with an increased water hyacinth mixing ratio. The cold gas efficiency and carbon conversion reached the maximum values of 77.64% and 69.9%, and the H_2 yield and H_2/CO ratio in the syngas improved to 0.34 Nm^3/kg and 1.62 under the water hyacinth mixing ratio of 0.75. This is attributed to the oxygen carrier being able to transfer most of the lattice oxygen in the bulk phase

through the oxygen vacancy to physical adsorption oxygen for gasification, according to the XPS characterization results. In addition, the generation of tar was reduced, the content of MAHs products in tar was increased, the content of NAHs products decreased, and the content of PAHs products first decreased and then increased with the increased hyacinth mixing ratio. This work is dedicated to exploring the synergistic properties on the microwave chemical looping gasification of PP plastic and water hyacinth in order to realize the synergistic resource utilization of multiple wastes and organic solid wastes to solve the environmental problems caused by improper disposal of wastes. It lays the foundation for further exploration of the continuous operation mechanism and reaction characteristics in a pilot-scale reactor in the future.

Author Contributions: F.A.: Methodology, Software, Investigation, Writing—original draft., D.C.: Investigation, Resources, Validation, Writing—review & editing, Data curation, W.M.: Writing—review, Formal analysis, Y.Y.: Writing—review, Formal analysis, D.S.: Methodology, Validation, Z.Z.: Resources, Writing—review & editing, Supervision, and X.W.: Conceptualization, Resources, Writing—review & editing, Supervision. All authors have read and agreed to the published version of the manuscript.

Funding: The project was financially supported by the Science and Technology Project of China Energy Science and Technology Research Institute Co., Ltd. (D2023Y01), and the National Key Research and Development Program of China (2020YFC1910000).

Institutional Review Board Statement: Not applicable.

Data Availability Statement: Data are contained within the article.

Conflicts of Interest: Author Fengxia An and Ying Yu was employed by China Energy Science and Technology Research Institute Co. Ltd. The remaining authors declare that the research was conducted in the absence of any commercial or financial relationships that could be construed as a potential conflict of interest.

Nomenclature

Abbreviation	
MAHs	Monocyclic aromatic hydrocarbons
NAHs	Naphthalene and bicyclic aromatic hydrocarbons
CLG	Chemical looping gasification
PP	Polypropylene
AR	Analytical reagent
SiC	Silicon carbide
GC-MS	Gas chromatography–mass spectrometry
Variables	
Y_i	Yield of each single gas component in the syngas, i = H_2, CO, CO_2, CH_4 (Nm^3/kg fuel)
V_{N_2}	N_2 flow rate at the inlet under room temperature (m^3/s)
X_i	Volume fraction of each single gas component measured online by the gas analyzer, i = H_2, CO, CO_2, CH_4 (%)
m_0	Total mass of fuel introduced to the reactor (kg)
Y_g	Total gas yield (Nm^3/kg fuel)
P_i	Relative portion of each single gas component in the gas product (%)
LHV	Lower heating value (MJ/Nm^3)
η_c	Carbon conversion rate (%)
CGE	Cold gas efficiency (%)
f_c	Mass fraction of carbon in the added fuel (%)
q_0	Low calorific value of the introduced fuel (MJ/kg)
H_2/CO	H_2/CO ratio in the gas product
CO/CO_2	CO/CO_2 ratio in the gas product

References

1. Stephen, J.L.; Periyasamy, B. Innovative developments in biofuels production from organic waste materials: A review. *Fuel* **2018**, *214*, 623–633. [CrossRef]
2. Iglinski, B.; Kujawski, W.; Kielkowska, U. Pyrolysis of Waste Biomass: Technical and Process Achievements, and Future Development—A Review. *Energies* **2023**, *16*, 1829. [CrossRef]
3. Hetland, J.; Yowargana, P.; Leduc, S.; Kraxner, F. Carbon-negative emissions: Systemic impacts of biomass conversion: A case study on CO_2 capture and storage options. *Int. J. Greenh. Gas Control* **2016**, *49*, 330–342. [CrossRef]
4. Ferreira, S.; Monteiro, E.; Brito, P.; Vilarinho, C. Biomass resources in Portugal: Current status and prospects. *Renew. Sustain. Energy Rev.* **2017**, *78*, 1221–1235. [CrossRef]
5. Condori, O.; García-Labiano, F.; de Diego, L.F.; Izquierdo, M.T.; Abad, A.; Adánez, J. Biomass chemical looping gasification for syngas production using ilmenite as oxygen carrier in a 1.5 kWth unit. *Chem. Eng. J.* **2021**, *405*, 126679. [CrossRef]
6. Samprón, I.; de Diego, L.F.; García-Labiano, F.; Izquierdo, M.T.; Abad, A.; Adánez, J. Biomass Chemical Looping Gasification of pine wood using a synthetic Fe_2O_3/Al_2O_3 oxygen carrier in a continuous unit. *Bioresour. Technol.* **2020**, *316*, 123908. [CrossRef]
7. Niu, Y.H.; Chi, Z.Y.; Li, M. Advancements in biomass gasification research utilizing iron-based oxygen carriers in chemical looing: A review. *Mater. Rep. Energy* **2024**, *4*, 100282. [CrossRef]
8. Ge, H.J.; Shen, L.H.; Feng, F.; Jiang, S.X. Experiments on biomass gasification using chemical looping with nickel-based oxygen carrier in a 25 kWth reactor. *Appl. Therm. Eng.* **2015**, *85*, 52–60. [CrossRef]
9. Sampron, I.; Purnomo, V.; Mattiósson, T.; Leion, H.; de Diego, L.F.; García-Labiano, F. Catalytic Activity of Oxygen Carriers on the Removal of Tar Byproducts for Biomass Chemical Looping Gasification Application. *Energy Fuels* **2023**, *37*, 16629–16638. [CrossRef]
10. Wei, G.Q.; He, F.; Zhao, Z.L.; Huang, Z.; Zheng, A.Q.; Zhao, K.; Li, H.B. Performance of Fe-Ni bimetallic oxygen carriers for chemical looping gasification of biomass in a 10 kWth interconnected circulating fluidized bed reactor. *Int. J. Hydrogen Energy* **2015**, *40*, 16021–16032. [CrossRef]
11. Liu, Q.R.; He, H.; Li, H.P.; Jia, J.B.; Huang, G.X.; Xing, B.L.; Zhang, C.X.; Cao, Y.J. Characteristics and kinetics of coal char steam gasification under microwave heating. *Fuel* **2019**, *256*, 115899. [CrossRef]
12. Li, J.; Tao, J.Y.; Yan, B.B.; Jiao, L.G.; Chen, G.Y.; Hu, J.L. Review of microwave-based treatments of biomass gasification tar. *Renew. Sustain. Energy Rev.* **2021**, *150*, 111510. [CrossRef]
13. Qi, H.Q.; Cui, P.Z.; Liu, Z.Q.; Xu, Z.F.; Yao, D.; Wang, Y.L.; Zhu, Z.Y.; Yang, S. Conceptual design and comprehensive analysis for novel municipal sludge gasification-based hydrogen production via plasma gasifier. *Energy Convers. Manag.* **2021**, *245*, 114635. [CrossRef]
14. Lian, M.L.; Li, S.; Wu, W.F.; Li, L.; Miao, Y.J.; Ge, Y. Graphite-assisted microwave carbon dioxide gasification of wet stalks. *Renew. Energy* **2023**, *219*, 119445. [CrossRef]
15. Ellison, C.; Abdelsayed, V.; Smith, M.; Shekhawat, D. Comparative evaluation of microwave and conventional gasification of different coal types: Experimental reaction studies. *Fuel* **2022**, *321*, 124055. [CrossRef]
16. Hu, M.T.; Deng, W.Y.; Su, Y.X.; Wang, L.H.; Chen, G. Production of hydrogen-rich syngas through microwave-assisted gasification of sewage sludge in steam-CO_2 atmosphere. *Fuel* **2024**, *357*, 129855. [CrossRef]
17. Ohnishi, T.; Kawakami, K.; Nishioka, M.; Ogura, M. Direct decomposition of NO on metal-loaded zeolites with coexistence of oxygen and water vapor under unsteady-state conditions by NO concentration and microwave rapid heating. *Catal. Today* **2017**, *281*, 566–574. [CrossRef]
18. Sulaiman, S.A.; Roslan, R.; Inayat, M.; Naz, M.Y. Effect of blending ratio and catalyst loading on co-gasification of wood chips and coconut waste. *J. Energy Inst.* **2018**, *91*, 779–785. [CrossRef]
19. Hu, M.; Gao, L.; Chen, Z.H.; Ma, C.F.; Zhou, Y.; Chen, J.; Ma, S.; Laghari, M.; Xiao, B.; Zhang, B.P.; et al. Syngas production by catalytic in-situ steam co-gasification of wet sewage sludge and pine sawdust. *Energy Convers. Manag.* **2016**, *111*, 409–416. [CrossRef]
20. Chattopadhyay, J.; Pathak, T.S.; Srivastava, R.; Singh, A.C. Catalytic co-pyrolysis of paper biomass and plastic mixtures (HDPE (high density polyethylene), PP (polypropylene) and PET (polyethylene terephthalate)) and product analysis. *Energy* **2016**, *103*, 513–521. [CrossRef]
21. Guo, S.H.; Wang, Z.W.; Chen, G.F.; Zhang, M.J.; Sun, T.L.; Wang, Q.; Du, Z.M.; Chen, Y.; Wu, M.G.; Li, Z.F.; et al. Co-pyrolysis characteristics of forestry and agricultural residues and waste plastics: Thermal decomposition and products distribution. *Process Saf. Environ. Prot.* **2023**, *177*, 380–390. [CrossRef]
22. Terry, L.M.; Wee, M.X.J.; Chew, J.J.; Khaerudini, D.S.; Darsono, N.; Aqsha, A.; Saptoro, A.; Sunarso, J. Catalytic co-pyrolysis of oil palm trunk and polypropylene with Ni-Mo/TiO_2 and Ni/Al_2O_3: Oil composition and mechanism. *Environ. Res.* **2023**, *224*, 115550. [CrossRef]
23. Al-Maari, M.A.; Ahmad, M.A.; Din, A.T.M.; Hassan, H.; Alsobaai, A.M. Co-pyrolysis of oil palm empty fruit bunch and oil palm frond with low-density polyethylene and polypropylene for bio-oil production. *Arab. J. Chem.* **2021**, *14*, 103282. [CrossRef]

24. Wang, Z.W.; Burra, K.G.; Lei, T.Z.; Gupta, A.K. Co-pyrolysis of waste plastic and solid biomass for synergistic production of biofuels and chemicals—A review. *Prog. Energy Combust. Sci.* **2021**, *84*, 100899. [CrossRef]
25. Yang, T.H.; Hu, K.M.; Li, R.D.; Sun, Y.; Kai, X.P. Cogasification of typical plastics and rice straw with carbon dioxide. *Environ. Prog. Sustain. Energy* **2015**, *34*, 789–794. [CrossRef]
26. Zhang, S.Q.; Yue, X.M.; Yin, Z.Y.; Pan, T.T.; Dong, M.J.; Sun, T.Y. Study of the co-pyrolysis behavior of sewage-sludge/rice-straw and the kinetics. *Proc. Int. Conf. Min. Sci. Technol.* **2009**, *1*, 661–666. [CrossRef]
27. Torquato, L.M.; Braz, C.E.M.; Ribeiro, C.A.; Capela, J.M.V.; Crespi, M.S. Kinetic study of the co-firing of bagasse-sludge blends. *J. Therm. Anal. Calorim.* **2015**, *121*, 499–507. [CrossRef]
28. Lahijani, P.; Zainal, Z.A.; Mohamed, A.R.; Mohammadi, M. Co-gasification of tire and biomass for enhancement of tire-char reactivity in CO_2 gasification process. *Bioresour. Technol.* **2013**, *138*, 124–130. [CrossRef]
29. Fu, W.M.; Zhang, Y.N.; Cao, W.T.; Zhao, W.K.; Li, B.X. Microwave-assisted chemical looping gasification of plastics for H2-rich gas production. *Chem. Eng. J.* **2024**, *499*, 156225. [CrossRef]
30. An, F.X.; Chen, D.L.; Zhong, Z.P.; Wang, X.J. Experimental investigation of the effect of microwave power on the chemical looping gasification of aquatic plant water hyacinth. *J. Energy Inst.* **2024**, *114*, 101537. [CrossRef]
31. Burra, K.G.; Gupta, A.K. Synergistic effects in steam gasification of combined biomass and plastic waste mixtures. *Appl. Energy* **2018**, *211*, 230–236. [CrossRef]
32. Nanda, S.; Okolie, J.A.; Patel, R.; Pattnaik, F.; Fang, Z.; Dalai, A.K.; Kozinski, J.A.; Naik, S. Catalytic hydrothermal co-gasification of canola meal and low-density polyethylene using mixed metal oxides for hydrogen production. *Int. J. Hydrogen Energy* **2022**, *47*, 42084–42098. [CrossRef]
33. Zheng, Y.W.; Li, D.H.; Pei, T.; Wang, J.D.; Liu, C.; Lu, Y.; Lin, X.; Li, J.R.; Zheng, Z.F. Mechanism of synergistic effects and kinetic analysis in bamboo-LDPE waste ex-situ catalytic co-pyrolysis for enhanced aromatic hydrocarbon production via CeZrAl and HZSM-5 dual catalyst. *J. Environ. Chem. Eng.* **2022**, *10*, 107479. [CrossRef]
34. Hognon, C.; Dupont, C.; Grateau, M.; Delrue, F. Comparison of steam gasification reactivity of algal and lignocellulosic biomass: Influence of inorganic elements. *Bioresour. Technol.* **2014**, *164*, 347–353. [CrossRef]
35. Ahmad, F.; Zhang, Y.; Fu, W.; Zhao, W.; Xiong, Q.; Li, B. Microwave-assisted chemical looping gasification of sugarcane bagasse biomass using Fe_3O_4 as oxygen carrier for H_2/CO-rich syngas production. *Chem. Eng. J.* **2024**, *501*, 157675. [CrossRef]

Disclaimer/Publisher's Note: The statements, opinions and data contained in all publications are solely those of the individual author(s) and contributor(s) and not of MDPI and/or the editor(s). MDPI and/or the editor(s) disclaim responsibility for any injury to people or property resulting from any ideas, methods, instructions or products referred to in the content.